GEOPHYSICAL RESEARCH LETTERS, VOL. 22, NO. 13, PAGES 1721-1724, JULY 1, 1995

Correlated observations of HCl and $ClONO_2$ from UARS and implications for stratospheric chlorine partitioning

A. E. Dessler[1], D. B. Considine[1] G. A. Morris[1], M. R. Schoeberl[1], J. M. Russell, III[2], A. E. Roche[3], J. B. Kumer[3], J. L. Mergenthaler[3], J. W. Waters[4], J. C. Gille[5], G. K. Yue[2]

Abstract. We present the first near-global set of correlated measurements of stratospheric HCl and $ClONO_2$ concentrations. These data, obtained from the Upper Atmosphere Research Satellite (UARS) between August 1992 and March 1993, are analyzed using the Goddard trajectory mapping technique. These data indicate that, between 20 and 30 km altitude and 60°N to 60°S latitude, total inorganic chlorine (Cl_y) is fairly evenly distributed between $ClONO_2$ and HCl, with HCl the slightly more dominant reservoir. The sum of UARS measurements of HCl and nighttime $ClONO_2$, which approximates Cl_y at these altitudes, closely agrees with Cl_y derived from a tracer-Cl_y relation originally derived from aircraft data, increasing confidence in the UARS data. Comparisons between these data and two-dimensional model results suggest that models underpredict $ClONO_2$ (overpredict HCl) near 20 km and overpredict $ClONO_2$ (underpredict HCl) near 30 km, although the 20-km underprediction is not as large as analyses of aircraft measurements have indicated.

Introduction

Standard models of the stratosphere predict that, with the exception of the perturbed polar vortices, half or more of stratospheric inorganic chlorine should be in the form of hydrochloric acid (HCl), with most of the rest being chlorine nitrate ($ClONO_2$). The relative abundance of HCl and $ClONO_2$ is a major factor in determining the effectiveness of stratospheric inorganic chlorine (Cl_y) in ozone destruction because photolysis of $ClONO_2$ yields ClO, the chlorine radical implicated in catalyzing ozone loss, while HCl is a comparatively benign form of chlorine. Therefore, a reliable determination of the relative abundance of HCl and $ClONO_2$ is central to understanding ozone destruction.

The lack of correlated, global measurements of HCl and $ClONO_2$ has prevented rigorous validation of model predictions of the partitioning between these two species. Simultaneous shuttle-based ATMOS measurements of HCl and $ClONO_2$ indicate that HCl is the dominant member of Cl_y between 20 and 30 km [Zander et al., 1990]. In contrast, NASA ER-2 aircraft measurements of mid- and high-latitude HCl concentrations by Webster et al. [1994; 1993] suggest that, near 20 km (~500 K potential temperature), only ~40% of Cl_y is HCl. Measurements of ClO and other trace species measured simultaneously with these ER-2 HCl data, however, imply that HCl makes up ~88% of Cl_y [Stimpfle et al., 1994].

The data used in these previous analyses, however, suffer from various shortcomings. Interpretation of the ER-2 data is hampered by limited altitude coverage, limited seasonal coverage, and the lack of a simultaneous $ClONO_2$ measurement. Interpretation of the ATMOS data is hampered by limited latitudinal and seasonal coverage. Due to the importance of the Cl_y family in catalyzing stratospheric ozone destruction, disagreements between the various measurements and photochemical theory are an important uncertainty in our understanding of the chemistry of stratospheric ozone. In this paper, we use Upper Atmosphere Research Satellite (UARS) measurements of key species obtained between August 1992 and March 1993 to investigate this issue. Our focus is on the 550, 650, and 800 K potential temperature surfaces (approximately 21, 24, and 30 km, respectively), and latitudes between 65°N and 65°S. This is a region of exceptional scientific interest because it holds the majority of the Earth's ozone. HCl is measured by the HALogen Occultation Experiment (HALOE); $ClONO_2$ is measured by the Cryogenic Limb Array Etalon Spectrometer (CLAES). Over this altitude range and time span, HCl data (version 17) have an estimated accuracy of ±15%, and $ClONO_2$ data (version 7) have an estimated accuracy of ±30%. These are estimates of the total systematic uncertainty of the measurements, and are determined from an analysis of retrieval algorithms, instrumental considerations, and comparisons with correlative measurements.

Analysis

The primary difficulty with comparing HALOE HCl and CLAES $ClONO_2$ data arises because the instruments do not make simultaneous measurements in the same location. In order to compare $ClONO_2$ and HCl measurements made at different locations and times, we use the Goddard trajectory mapping technique [Morris et al., 1995]. Briefly, for each day on which there are HCl measurements, maps of $ClONO_2$ are made at noon and midnight (GMT). The maps are constructed from nighttime CLAES $ClONO_2$ measurements made within ±3 days and isentropically advected forward or backward to the time of the map using NMC balanced winds. Each HALOE HCl measurement made during the day is isentropically advected forward for up to twelve hours until the time of the next $ClONO_2$ map (either noon or midnight, GMT). Those $ClONO_2$ measurements within 400 km of the HCl measurement and in air with similar potential vorticity (PV) are considered

[1]NASA Goddard Space Flight Center
[2]NASA Langley Research Center
[3]Lockheed Palo Alto Research Laboratories
[4]Jet Propulsion Laboratory
[5]NCAR

Paper number 95GL01593
0094-8534/95/95GL-01593$03.00

correlated with the HCl observation. At 550, 650, and 800 K, the maximum allowable PV gradient between the $ClONO_2$ and HCl data is 1.7, 2.0, and 8.0×10^{-5} m^2 K s^{-1} kg^{-1}, respectively. Because of possible complications caused by the diurnal cycle of $ClONO_2$, we restrict our analysis to nighttime $ClONO_2$ data (solar zenith angles greater than 100°). Note that nighttime $ClONO_2$ is approximately the sum of daytime $ClONO_2$, ClO, and Cl. Because its lifetime is much longer than one day at these levels, HCl has no significant diurnal cycle. Each of the time periods discussed in this paper (August 18 to September 19, 1992, November 1 to 27, 1992, and February 12 to March 16, 1993), included ~20,000 nighttime $ClONO_2$ observations and ~700 HCl observations, and produced ~300 correlated observations each.

Figure 1 shows the sum of HCl and nighttime $ClONO_2$ as a function of latitude for the three potential temperature levels and three time periods. The error bars are representative of the accuracy of the sum of UARS data, ~±17%. The latitude coverage during a given time period is determined by the overlap of the HALOE and CLAES viewing patterns. On the 550 and 650 K surfaces, HCl and nighttime $ClONO_2$ together make up virtually all of Cl_y. On the 800 K surface, the sum of HCl and nighttime $ClONO_2$ make up at least 90% of Cl_y, with HOCl making up the rest. Thus, Fig. 1 can be considered to a good approximation to be a plot of Cl_y vs. latitude. Also shown on the plot is Cl_y derived from a Cl_y-tracer relation (solid line) based on aircraft data [Woodbridge et al., 1995] using zonally averaged measurements of CH_4 from HALOE. The UARS Cl_y agreement agrees well with derived Cl_y, adding confidence in the accuracy of the UARS data over this time period and altitude range.

To understand the partitioning of Cl_y between HCl and $ClONO_2$, we consider the ratio $[ClONO_2]/[HCl]$ (where [x] denotes the species concentration). Because there is no direct chemical reaction linking the molecules HCl and $ClONO_2$, we expand this ratio in terms of the ratios of constituents that are directly related by chemical reactions,

$$\frac{[ClONO_2]}{[HCl]} = \frac{[ClONO_2]}{[ClO]} \frac{[ClO]}{[Cl]} \frac{[Cl]}{[HCl]} \quad (1)$$

Assuming steady-state conditions, Equation (1) can be rewritten,

$$\frac{[ClONO_2]}{[HCl]} \cong \frac{k_{ClO+NO2}[NO_2]}{J_{ClONO2}} \times \frac{k_{Cl+O3}[O_3]}{(k_{ClO+O}[O]+k_{ClO+NO}[NO])} \frac{k_{HCl+OH}[OH]}{k_{CH4+Cl}[CH_4]} \quad (2)$$

where k denotes a bimolecular rate constant and J denotes a photolysis rate constant; unimportant terms, such as heterogeneous reactions involving $ClONO_2$, have been neglected. In the region of the atmosphere of interest, we note that $k_{ClO+NO}[NO] >> k_{ClO+O}[O]$, and subsequently substituting the steady-state relation ($k_{NO+O3}[O_3]$ +

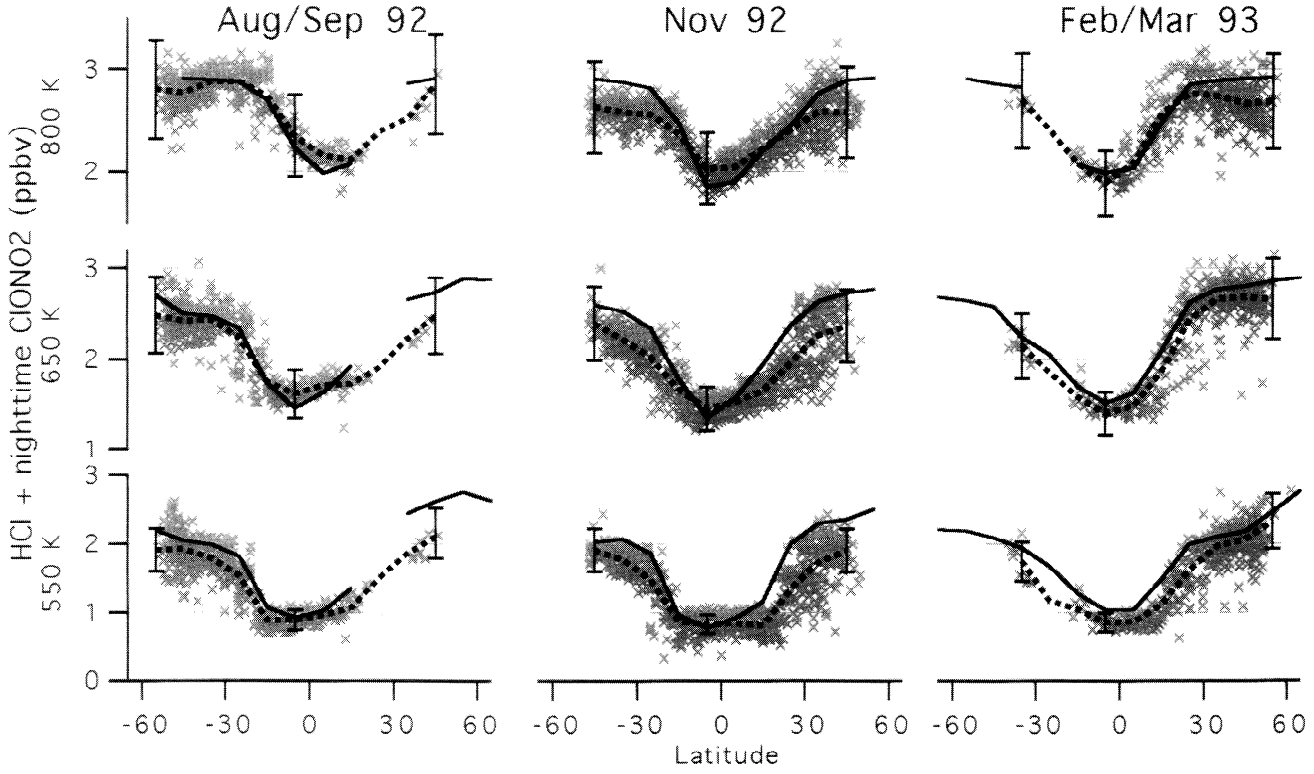

Figure 1. The sum of HCl and nighttime $ClONO_2$ (parts per billion by volume) vs. latitude. The individual UARS measurements (x) and an average of the UARS measurements (dashed lines) are both shown. Error bars are estimates of the accuracy of the UARS sum (±17%). The solid line is Cl_y derived from the relationship of Woodbridge et al. [1995] using zonally averaged HALOE measurements of CH_4 taken over the same time period that the chlorine data were obtained. The top row is the 800 K potential temperature surface, middle row is the 650 K surface, bottom row is the 550 K surface. The left column data are from August and September 1992, the middle column data are from November 1992, the right column data are from February and March 1993. On the 550 and 650 K surfaces these two constituents make up virtually all of Cl_y. On the 800 K surface, the sum makes up ~90% of Cl_y.

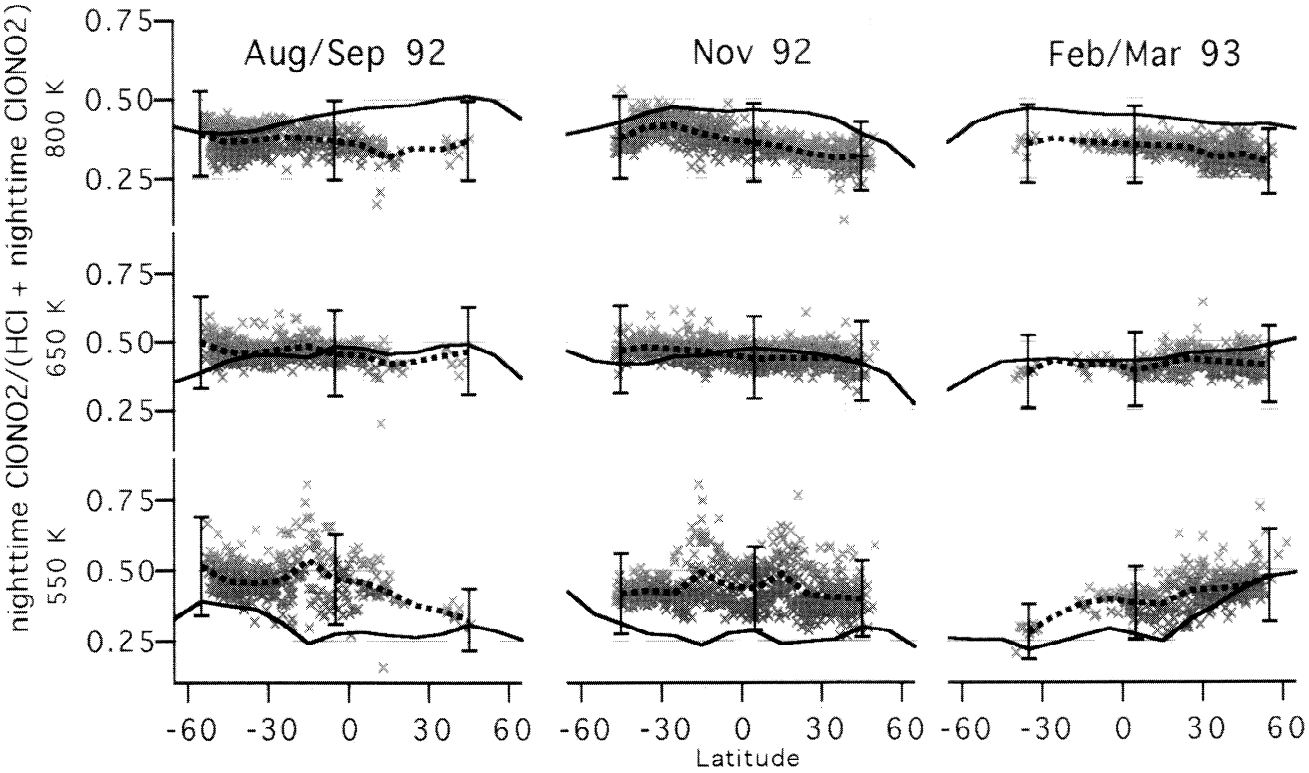

Figure 2. [nighttime $ClONO_2$]/([HCl]+[nighttime $ClONO_2$]) vs. latitude. The individual UARS measurements (x) and an average of the UARS measurements (dashed lines) are both shown. Error bars are estimates of the accuracy of the UARS ratio (±34%). The solid lines are calculations from the Goddard 2D model. The top row is the 800 K potential temperature surface, the middle row is the 650 K surface, and the bottom row is the 550 K surface. The left column data are from August and September 1992, the middle column data are from November 1992, the right column data are from February and March 1993.

$k_{NO+ClO}[ClO])/J_{NO2}$ for $[NO_2]/[NO]$, we obtain the expression,

$$\frac{[ClONO_2]}{[HCl]} \cong \frac{k_{ClO+NO2}}{J_{ClONO2}} \times \frac{\left(k_{Cl+O3}k_{NO+O3}[O_3]^2 + k_{Cl+O3}k_{NO+ClO}[ClO][O_3]\right)}{k_{ClO+NO}J_{NO2}} \times \frac{k_{HCl+OH}[OH]}{k_{CH4+Cl}[CH_4]} \quad (3)$$

Strictly speaking, Equation (3) is the ratio of daytime $ClONO_2$ to HCl. Because [ClO] << [$ClONO_2$] in this region of the atmosphere, this daytime ratio is expected to be both numerically similar to the ratio of [nighttime $ClONO_2$]/[HCl] and show similar dependencies on other atmospheric constituents. Over this region of the atmosphere, $k_{ClO+O3}k_{NO+O3}[O_3]^2$ is several orders of magnitude larger than $k_{Cl+O3}k_{NO+ClO}[ClO][O_3]$ at 550 K, decreasing to about five times larger at 800 K. Thus, the ratio in (3) is approximately quadratically dependent on $[O_3]$, linearly dependent on [OH] and $[CH_4]$, and less sensitive to changes in [ClO]. Changes in other atmospheric parameters, such as sulfate aerosol surface area or the abundance of NO_X (NO_X = NO + NO_2), only perturb the partitioning of $ClONO_2$ and HCl through their impact on the concentrations of O_3, ClO, OH, or CH_4.

Figure 2 plots the quantity [nighttime $ClONO_2$]/([HCl] + [nighttime $ClONO_2$]), approximately the fraction of Cl_y that is in the form of nighttime $ClONO_2$. Note that this quantity is related to Equation (3) by: [nighttime $ClONO_2$]/([HCl]+[nighttime $ClONO_2$]) = 1 - 1/(1 + [nighttime $ClONO_2$]/[HCl]). Over the conditions considered in this analysis, these ratios react similarly to changes in the parameters on the right hand side of Equation (3). The accuracy of the ratio of the UARS data is ±34%. These data suggest that Cl_y is fairly evenly distributed between $ClONO_2$ and HCl, with HCl the slightly more dominant reservoir, over the range of potential temperatures, latitudes, and time considered in this paper.

On the 550 K surface, the August and September 1992 and February and March 1993 data are mirror images of each other, as expected since they represent the same season in opposite hemispheres. These data also show an interhemispheric gradient, with the fraction of Cl_y in nighttime $ClONO_2$ varying from ~0.5 in the winter hemisphere to ~0.3 in the summer hemisphere. In between these two time periods, the November 1992 data show no interhemispheric gradient, with the fraction of Cl_y in nighttime $ClONO_2$ approximately ~0.4 over the entire range between 60°N and 60°S. On the 650 K surface, the ratio is between 0.4 and 0.5 in all three time periods, with virtually no gradient. On the 800 K surface, the ratio is 0.3 to 0.4 in all three time periods, also with virtually no gradient.

The solid lines in Fig. 2 are [nighttime $ClONO_2$]/([HCl] + [nighttime $ClONO_2$]) from the Goddard two-dimensional (2D) fixed transport model [e.g., Considine et al., 1994, and references therein]. The model includes sulfate heterogeneous reactions using the formulation of Hanson and Ravishankara [1994], and reaction rates

and cross sections from DeMore et al. [1994]. Daytime-averaged photolysis coefficients are obtained from a tabulation of off-line calculations using the radiation code of Anderson and Lloyd [1990]. The table values agree well with the calculated values for all wavelengths, overhead column O_3 amounts, and solar zenith angles [R. Kawa, private communication, 1995].

In order to make the comparison between the model and the UARS data more meaningful, the model has been constrained using UARS observations. At each time step, measurements of N_2O and CH_4 from CLAES (version 7), O_3 (205 GHz), H_2O, and temperature from MLS (version 3), and aerosol surface area density derived from SAGE II [Yue et al., 1994] are inserted into the corresponding model fields. The remaining model constituents are subject to model transport (using a climatological circulation) and model chemistry, and so relax to values consistent with both the model formulation and the observations. Incorporating measured O_3 produced the largest improvement when used as a constraining field, consistent with the quadratic dependence of the partitioning on O_3 in Eq. (3).

Over virtually the entire range of altitude and time covered in this analysis, the partitioning of Cl_y in the 2D model (solid line) and in the UARS measurements (dotted line) agree within the accuracy error bars of the measurements. At 550 K, however, the model tends to systematically overpredict HCl (and underpredict nighttime $ClONO_2$). The discrepancy is similar in sign but of smaller magnitude than that seen in the ER-2 data [Salawitch et al., 1994]. On the 650 K surface, the agreement between measured and predicted Cl_y partitioning is excellent. On the 800 K surface, the model tends to systematically underpredict HCl (and overpredict nighttime $ClONO_2$), a discrepancy which is opposite in sign to the disagreement on the 550 K surface. A similar difference has been previously identified in the ATMOS data near 800 K [e.g., Natarajan and Callis, 1991].

Analyses of previous *in situ* measurements of ClO between 20 and 30 km altitude [Dessler et al., 1993; Avallone et al., 1993] show a pattern consistent with our analysis. Models of these data tend to underpredict ClO around 20 km and overpredict ClO near 30 km. This is consistent with an underlying underprediction of $ClONO_2$ (overprediction of HCl) by the model at 20 km and overprediction of $ClONO_2$ (underprediction of HCl) near 30 km, a disagreement similar to our analysis. In fact, as pointed out by Avallone et al. [1993], their 20-km ClO data are consistent with HCl making up about ~60% of Cl_y instead of the ~80% that standard photochemical models predict. Our data suggests that HCl does indeed make up ~60% of Cl_y near 20 km and at the latitude and time of year of the Avallone et al. balloon flight (although the 1991 balloon flight experienced much lower aerosol surface area density). This underprediction of $ClONO_2$ (overprediction of HCl) by the model at 20 km is also consistent with the known underprediction of the OH radical by models incorporating standard photochemistry [Salawitch et al., 1994].

Conclusions

We have analyzed the first near-global set of correlated measurements of HCl and $ClONO_2$ concentrations. These data provide the most rigorous indication that, between 20 and 30 km altitude and 60°N to 60°S latitude, total inorganic chlorine (Cl_y) is fairly evenly distributed between $ClONO_2$ and HCl, with HCl the slightly more dominant reservoir. We conclude that models incorporating standard photochemistry underpredict $ClONO_2$ (overpredict HCl) near 20 km and overpredict $ClONO_2$ (underpredict HCl) near 30 km. However, the discrepancy at 550 K (~21 km), near the ER-2 flight altitude, is not as significant as suggested by *in situ* measurements of HCl of Webster et al. [1994; 1993] Our conclusions, predicated on UARS measurements, are consistent with previous satellite observations of HCl and $ClONO_2$ and *in situ* measurements of ClO.

Acknowledgments. We thank Drs. A. R. Douglass, L. Froidevaux, J. F. Gleason, S. R. Kawa, and R. S. Stolarski for helpful comments. AED was supported by a National Research Council postdoctoral fellowship.

References

Anderson, D. E., Jr., and S. A. Lloyd, Polar Twilight UV-Visible Radiation Field: Perturbations due to Multiple Scattering, Ozone Depletion, Stratospheric Clouds, and Surface Albedo, *J. Geophys. Res., 95,* 7429-7434, 1990.

Avallone, L. M. et al., Balloon-borne In Situ Measurements of ClO and Ozone: Implications for Heterogeneous Chemistry and Mid-Latitude Ozone Loss, *Geophys. Res. Lett., 20,* 1795-1798, 1993.

Considine, D. B., A. R. Douglass, and C. H. Jackman, Effects of a Polar Stratospheric Cloud Parameterization on Ozone Depletion due to Stratospheric Aircraft in a Two-Dimensional Model, *J. Geophys. Res., 99,* 18,879-18,894, 1994.

DeMore, W. B. et al., Chemical Kinetics and Photochemical Data for Use in Stratospheric Modeling - Evaluation Number 11, JPL, Publication 94-26, 1994.

Dessler, A. E. et al., Balloon-borne Measurements of ClO, NO, and O_3 in a Volcanic Cloud: An Analysis of Heterogeneous Chemistry Between 20 and 30 km, *Geophys. Res. Lett., 20,* 2527-2530, 1993.

Hanson, D. R., and A. R. Ravishankara, Reactive Uptake of $ClONO_2$ Onto Sulfuric Acid Due to Reaction with HCl and H_2O, *J. Phys. Chem., 98,* 5728-5735, 1994.

Morris, G. A. et al., Trajectory Mapping of Upper Atmosphere Research Satellite (UARS) Data, *J. Geophys. Res., In Press,* 1995.

Natarajan, M., and L. B. Callis, Stratospheric Photochemical Studies With Atmospheric Trace Molecule Spectroscopy (ATMOS) Measurements, *J. Geophys. Res., 96,* 9361-9370, 1991.

Salawitch, R. J. et al., The Distribution of Hydrogen, Nitrogen, and Chlorine Radicals in the Lower Stratosphere: Implications for Changes in O_3 Due to Emission of NO_y From Supersonic Aircraft, *Geophys. Res. Lett., 21,* 2547-2550, 1994.

Stimpfle, R. M. et al., The Response of ClO Radical Concentrations to Variations in NO_2 Radical Concentrations in the Lower Stratosphere, *Geophys. Res. Lett., 21,* 2543-2546, 1994.

Webster, C. R. et al., Hydrochloric Acid and the Chlorine Budget of the Lower Stratosphere, *Geophys. Res. Lett., 21,* 2575-2578, 1994.

Webster, C. R. et al., Chlorine Chemistry on Polar Stratospheric Cloud Particles in the Arctic Winter, *Science, 261,* 1130-1134, 1993.

Woodbridge, E. L. et al., Estimates of Total Organic and Inorganic Chlorine in the Lower Stratosphere From in situ and Flask Measurements During AASE II, *J. Geophys. Res., 100,* 3057-3064, 1995.

Yue, G. K., L. R. Poole, P.-H. Wang, and E. W. Chiou, Stratospheric Aerosol Acidity, Density, and Refractive Index Deduced From SAGE II and NMC Temperature Data, *J. Geophys. Res., 99,* 3727-3738, 1994.

Zander, R., M. R. Gunson, J. C. Foster, C. P. Rinsland, and J. Namkung, Stratospheric $ClONO_2$, HCl, and HF Concentration Profiles Derived From Atmospheric Trace Molecule Spectroscopy Experiment Spacelab 3 Observations: An Update, *J. Geophys. Res., 95,* 20,519-20,525, 1990.

Corresponding author: A. E. Dessler, NASA Goddard Space Flight Center, Code 916, Greenbelt, MD 20771 (e-mail: dessler@maia.gsfc.nasa.gov)

(Received February 15, 1995; revised April 20, 1995; accepted May 16, 1995)